

Dynamic Monitoring of Structural Deformations utilizing an Experimentally Validated Efficient Technique

Khalid L. A. El-Ashmawy

Civil Engineering Department, College of Engineering and Islamic Architecture, Umm Al-Qura University, Saudi Arabia
klashmawy@uqu.edu.sa (corresponding author)

Mohamed A. El Zareef

Civil Engineering Department, College of Engineering and Islamic Architecture, Umm Al-Qura University, Saudi Arabia | Structural Engineering Department, Faculty of Engineering, Mansoura University, Egypt
mzareef76@mans.edu.eg

Received: 10 February 2023 | Revised: 1 March 2023 and 17 March 2023 | Accepted: 19 March 2023

Licensed under a CC-BY 4.0 license | Copyright (c) by the authors | DOI: <https://doi.org/10.48084/etasr.5772>

ABSTRACT

Up-to-date detection of a building's responses under various load situations is essential to generate data used to assess its capacity to bear crucial loads. This study presents an innovative and effective method to detect structural displacements and provide a more accurate alternative to existing approaches such as trigonometry leveling and angle intersecting. The least squares method was used to produce a concurrent solution that includes all the observed data to improve precision and retrieve the data needed for statistical analysis. The proposed method was validated experimentally and compared with the total station, conventional structural analysis, and displacement gauges to test and monitor a three-point loaded Reinforced Concrete (RC) beam at seven discrete points. The displacement gauge measurements were used as a baseline for comparing the outcomes from the other methods. The maximum mid-span deflection of the tested RC beam showed that the variation between the recorded displacement using displacement gauges and the suggested approach was below 0.31mm, resulting in a 3.7% inaccuracy, while the total station observations and the ACI-Code deflection provisions provided deflections of 0.62 and 3.64mm, resulting in 7.4% and 43.4% inaccuracies, respectively. Furthermore, comparing the results using root-mean-square error, the suggested method's precision in detecting displacements was much superior to the total station. The proposed approach was effective for detecting horizontal and vertical deformations and offers a viable option for building monitoring across both the element and whole building stages.

Keywords-structural deformation; structure monitoring; ACI deflection provisions; total-station; angle-intersecting method

I. INTRODUCTION

Dynamic monitoring deals with the identification of the change of a member's location, dimension, and geometry for its specified shape. The purpose of identifying deformations is to evaluate not just the precise position of the detected member, but additionally its fluctuation over a period to avoid the collapse of massive buildings. National authorities are very concerned about dynamic building monitoring as a way to manage the structural safety and stability of bridges, tunnels, high-rise buildings, and other public structures [1]. Various survey techniques have been proposed to assist in building surveillance and detect deformations at different locations [1]. In this case, finding an accurate, affordable, reliable, and time-saving 3D measuring method is challenging. Although such

demands can be achieved in many ways [1-3], it is challenging to find an approach that satisfies all the criteria mentioned above. In the field of structural measurement, topographic techniques that rely on height differences, observed angles, and lengths are often utilized [4-6]. For this purpose, total stations, electronic distance measurement instruments, and theodolites are just examples of the various devices used [7-8], while indirect approaches such as single- or multi-intersections and precise leveling traverse are employed for difficult-to-reach locations [6, 10-11]. Contact sensors can also be used for these observations, such as inclinometers, dial-gauges, pendulums, or extensometers [1-3, 12], but due to their nature, they cannot be used in the last phases of the destructive loading test but can capture only one-dimensional measurements. The Global Positioning System (GPS) is used in building monitoring in

conjunction with other sensors [7, 13-16], but has two fundamental restrictions: it cannot be used inside or under barriers and its current accuracy is restricted to +/-10mm in the horizontal direction and +/-20mm in the vertical direction [10]. The photogrammetric close-range technology is also used for monitoring structural deformation [17-20]. In [17], high-accuracy measurements were produced using digital close-range photogrammetry. This approach provided quick, remote, spatial data collecting with images that provided a long-term visual record. Using targets may not always be appropriate, particularly if access to the object is difficult or hazardous. To determine the scale definition in the photogrammetric procedure, observations made with extra devices, such as reflectorless total stations, are needed. Novel approaches and computational methods for building monitoring were reported in the Terrestrial Laser Scanning (TLS) method [21]. Although these methods had improved precision and were reliable for structural monitoring [22], they have not been validated in more complicated structures such as tunnels and high-rise buildings. The stated inspection focuses primarily on the stability and precision of georeferencing which serves as the base for comparing various scans and the point-cloud-based displacement determination [21]. Various types of surfaces such as mesh and polynomial, and resample-point-cloud have been typically used in comparison [23-24].

This study proposes a novel approach based on a numerical model to determine the ground coordinates from observations at individual monitoring locations and modifies duplicated observations whose accuracy may be assessed by a least squares solution. This method was used for the displacement detection of a reinforced concrete beam at various load steps and the results were compared to those of ACI 318-19 [25], total-station, and displacement gauge.

II. THE MATHEMATICAL MODEL

Figure 1 shows the layout for finding the missing coordinates (x_c, y_c, z_c) of node C. Node A represents the device location, node B is the back-sight location, and their respective known ground coordinates are (x_A, y_A, z_A) and (x_B, y_B, z_B).

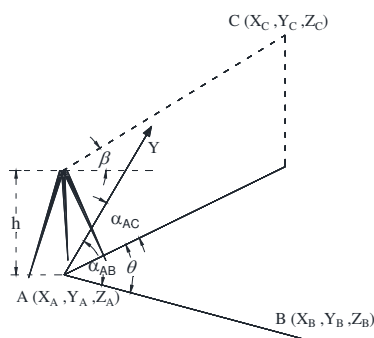


Fig. 1. Geometric representation of the proposed model.

The observation equations of the observed horizontal angle θ and the vertical angle β are given by [26]:

$$v_{\theta} + \left(\frac{Y_C - Y_A}{AC^2}\right) \Delta X_C + \left(\frac{X_A - X_C}{AC^2}\right) \Delta Y_C = \quad (1)$$

$$T \tan^{-1} \left(\frac{X_B - X_A}{Y_B - Y_A}\right)_o - T \tan^{-1} \left(\frac{X_C - X_A}{Y_C - Y_A}\right)_o - \theta$$

and:

$$v_{\beta} + \frac{g \times (X_C - X_A)}{AC(AC^2 + g^2)} \Delta X_C + \frac{g \times (Y_C - Y_A)}{AC(AC^2 + g^2)} \Delta Y_C + \frac{-AC}{(AC^2 + g^2)} \Delta Z_C = T \tan^{-1} \left(\frac{g}{AC}\right)_o - \beta \quad (2)$$

where:

$$AC^2 = (X_C - X_A)^2 + (Y_C - Y_A)^2,$$

$$g = Z_C - Z_A - h,$$

and h is the instrument height. Finding the ground coordinates of point C requires three observations and the solution of three observation formulas, while a least squares solution would be feasible if there are more than three observations [27].

III. DEFLECTION ANALYSIS OF THE TESTED RC BEAM

Due to its importance as a key performance parameter, many studies investigated the deflection of structural elements and the factors that influence it, such as element length to depth ratio, shrinkage of concrete, creep of concrete, fiber content, fire stresses, and aggregate size [28-38]. According to ACI 318-19 [25], the moment at the first crack (M_{cr}) can be determined based on the concrete modulus of rupture (f_r) and ignoring the impact of steel bars in computing the gross moment of inertia (I_g). Consequently, the cracked distributed load (W_{cr}) of the tested beam can be calculated as follows.

$$W_{cr} = 8 \times 0.62 \sqrt{f'_c} \times \frac{bt^2}{6l^2} \quad (3)$$

The self-weight of the tested beam is less than the cracked distributed load (W_{cr}). For the applied levels of concentrated load (P), the applied moment (M_a) including the beam's self-weight (W_{ow}) would be more than the beam's cracked moment. As a result, I_g can be used to calculate the deflection due to beam self-weight (δ_{ow}), while the effective moment of inertia (I_e) will be applied when computing deflection due to self-weight plus the applied concentrated load (δ_{ow+P}). The self-weight deflection (δ_{ow}) and all applied load deflections (δ_{ow+P}) is given by:

$$\delta_{ow+P} = \frac{5 W_{ow} l^4}{384 E I_{e(ow+P)}} + \frac{P l^3}{48 E I_{e(ow+P)}} \quad (4)$$

Under the application of all loads and according to ACI 318-19 [25], the effective moment of inertia (I_{e(ow+P)}) can be computed as follows, when the applied moment (M_a) exceeds the two-thirds of the cracked moment (0.67M_{cr}):

$$I_{e(ow+P)} = I_{cr} / \left[1 - \left(\frac{2}{3} \frac{M_{cr}}{M_a}\right)^2 \left(1 - \frac{I_{cr}}{I_g}\right) \right] \quad (5)$$

The deflection results of (4) under different concentrated load levels (15, 20, 25, and 30kN) were used in comparison with other deflection values obtained from the total station, and displacement gauges (LVDT) methods.

IV. EXPERIMENTAL WORK AND TEST SET-UP

The proposed mathematical model for detecting deformations can be used for all types of structures, bridges, and elements. This model was used to detect the structural deformability of a three-point loaded reinforced concrete beams. The compressive strength of the cylinder concrete at 28 days was 30MPa, and the beam was 350mm in depth and 150mm in width. As shown in Figure 2, the beam had two supports and one mid-span point load with a main span (L) of 4m. One concentrated load was applied at the mid-span of the beam with four different levels (15, 20, 25, and 30kN). Deflection values were measured at 7 distinct locations: $L/8$, $L/4$, $3L/8$, $L/2$, $5L/8$, $3L/4$, and $7L/8$. At each deflection point, a paper prism and LVDT were attached to detect deflection values. The beam had a flexural reinforcement of 3T12 with a steel yield strength of 420MPa.

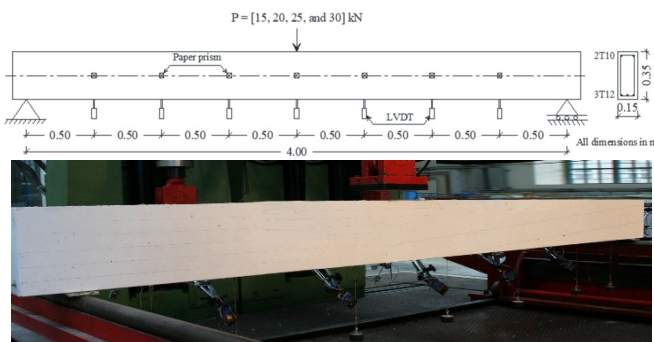


Fig. 2. Test set-up and deflection point locations for the tested beam

Two observation stations were placed at the test platform, 5m apart from the beam, and the most well-known and widely approved approach for determining level differences in the field was adopted. Level variations could be monitored using a single level, as well as measurements on the invar-rods utilizing 2 distinct equipment horizons. This method is closely related to ensuring the appropriate accuracy required to measure field-level differences [8, 39]. The accurate leveling of a GPLE3 geodetic invar rod with 10mm graduation and a Leica NA2 automated leveling with a Leica (10mm) GPM3 parallel plate micrometer adapter was used to obtain the level variance between the two monitoring locations. A Topcon GTS710 total station was used to assess the horizontal length separating the two monitoring sites. Six horizontal distances (3 direct and 3 reversed distances) were measured, and their mean was used to calculate the final horizontal distance. A local coordinate system was assigned to the coordinates of the 2 observation (control) stations after the horizontal and height distances between the two monitoring stations were determined.

The deflection points on the tested beam were measured before and after each load step. The deflection points were measured using a Wild (Leica) T2. The horizontal angles to the deflection points were determined using direction and closing the horizon procedures and detecting the horizontal circles across the left and right sides. Multiple angles were measured using the circle advanced before each reading to mitigate systemic faults. The angles of every observation were

determined and the end value of the horizontal angle was taken as the mean of all measurements. The vertical angles for the deflection points were determined by reading and averaging the vertical circles on the left and right. For each deflection point, the vertical angle was determined by taking the mean of the vertical circle's measurements on both the left and right faces. The deflection points' coordinates were observed using a Topcon GTS710 total station. It should be noted that the devices were properly verified and confirmed to be in a good condition before carrying out the measurements.

V. RESULTS AND DISCUSSION

The deflections of a simple-span RC beam exposed to the point loading steps were used as a serviceability evaluation criterion. Deflection observations using LVDT gauges at the defined points of the tested RC beam were used for comparison at each loading stage. Figure 3 and Table I show the detected deflections of various deflection locations at each load step for the proposed, the total station, and the ACI 318-19 [25] methods. The deflection derived from the proposed model had the best correlation with that obtained using LVDT gauges, with an RMSE of 0.09 at the low, 0.19 at the high, and 0.17 for all observation points and loading stages. The deflection results obtained using the total station and ACI 318-19 [25] were less accurate and conservative when compared to the results of LVDT gauges. The RMSE ranged from 0.23 at the low and 0.52 at the high loading stages, with an overall RMSE of 0.42 based on discrepancies between the total station and LVDT gauges. However, for safety concerns, the deflection results using ACI 318-19 [25] were substantially conservative when compared to those of LVDT gauges, with an RMSE ranging from 1.95 at the low to 1.75 at the high loading stage and an overall RMSE of 1.86. In comparison to the LVDT results, the deflection results of the proposed mathematical model were more accurate than those of the total station.

VI. CONCLUSION

The proposed method adds a new dimension to the methods of angle intersection and trigonometric leveling. This method uses the least-squares solution to produce a response that includes multiple measurements in a single operation. This improves the predicted precision and provides the information needed in descriptive statistics. Based on an experimental and analytical analysis of a three-point-loaded, simply supported, reinforced-concrete beam, this method is proposed for reliably measuring structural element deformation, drawing the following conclusions in comparison to the typical approaches employed for this purpose:

- The proposed mathematical model outperformed the established approaches in assessing structural element deformation in terms of precision, feasibility, timesaving, and economy.
- The proposed model's results were most tightly correlated to the experimental results obtained using LVDT gauges.
- The proposed model produced more-accurate results compared to the total station.

- The proposed approach offered high accuracy even when compared to the ACI 318-19 deflection provisions.
- The results showed a strong correlation with the LVDT gauge results, with an overall RMSE of less than 0.17. The

respective RMSEs for the total station and ACI 318-19 were 0.42 and 1.86.

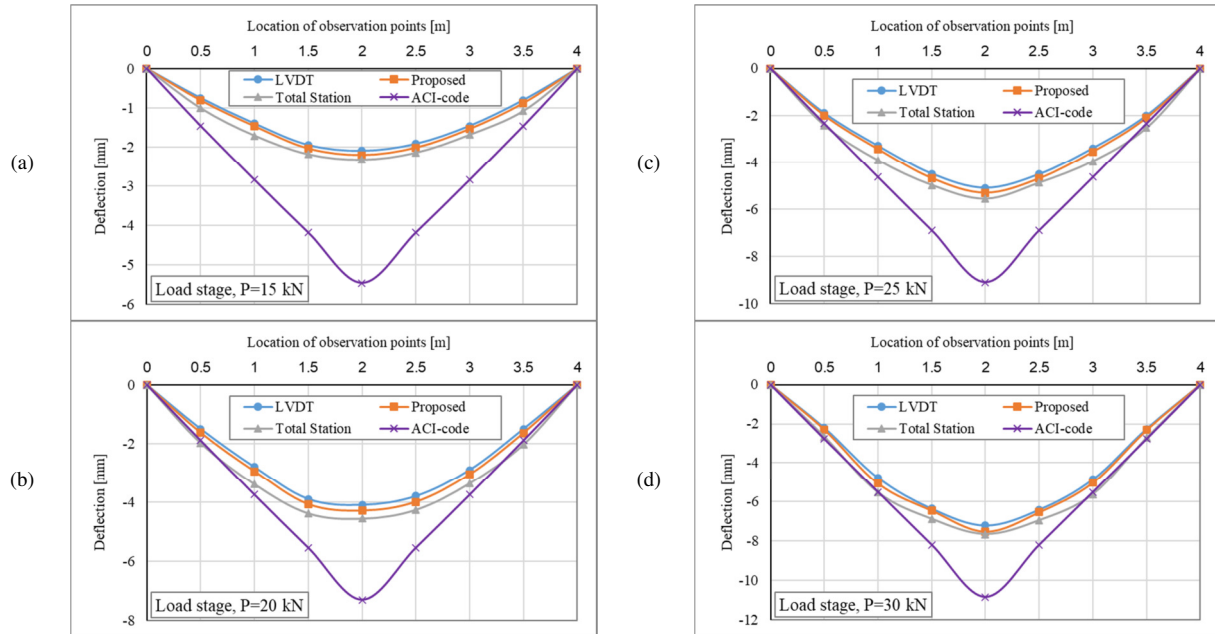


Fig. 3. Deflection of the tested beam at different stages of loading using LVDT, proposed model, total station, and ACI 318-19.

TABLE I. COMPARISON OF VERTICAL DEFLECTIONS AND DISCREPANCIES USING DIFFERENT METHODS

Step of loading	Observation method		1/8	1/4	3/8	1/2	5/8	3/4	7/8	RMSE	RMSE (for all loading steps)	
Step I (15kN)	LVDT	Deflection	0.75	1.47	2.21	2.76	2.22	1.46	0.8			
		Proposed method	Deflection	0.81	1.57	2.31	2.83	2.33	1.58	0.88		
	Total station	Deflection	1.01	1.71	2.45	2.95	2.46	1.69	1.02			
		Discrepancies	0.26	0.24	0.24	0.19	0.24	0.23	0.22	0.23	0.23	0.42
	ACI 318-19	Deflection	1.46	2.85	4.19	5.47	4.19	2.85	1.46			
		[22]	Discrepancies	0.71	1.45	2.24	3.37	2.27	1.39	0.66	1.95	1.86
Step II (20kN)	LVDT	Deflection	1.5	2.8	3.9	4.59	3.8	2.9	1.5			
		Proposed method	Deflection	1.63	2.95	4.08	4.79	4	3.06	1.64		
	Total station	Deflection	1.85	3.2	4.38	5.05	4.26	3.26	1.86			
		Discrepancies	0.13	0.15	0.18	0.2	0.2	0.16	0.14	0.17	0.17	
	ACI 318-19	Deflection	1.9	3.76	5.55	7.31	5.55	3.76	1.9			
		[22]	Discrepancies	0.4	0.96	1.65	3.21	1.75	0.86	0.4	1.61	
Step III (25kN)	LVDT	Deflection	1.9	3.3	5.15	6.41	5.17	3.4	2			
		Proposed method	Deflection	2	3.59	5.34	6.62	5.35	3.63	2.1		
	Total station	Deflection	2.32	3.92	5.49	6.87	5.53	3.96	2.41			
		Discrepancies	0.42	0.62	0.34	0.46	0.36	0.56	0.41	0.46	0.46	
	ACI 318-19	Deflection	2.34	4.64	6.89	9.09	6.89	4.64	2.34			
		[22]	Discrepancies	0.44	1.34	2.39	3.99	2.37	1.24	0.34	2.10	
Step IV (30kN)	LVDT	Deflection	2.2	4.77	6.94	8.39	6.98	4.85	2.25			
		Proposed method	Deflection	2.29	5.06	7.04	8.7	7.12	5.02	2.32		
	Total station	Deflection	2.65	5.39	7.4	9.01	7.43	5.38	2.71			
		Discrepancies	0.09	0.29	0.1	0.31	0.14	0.17	0.07	0.19	0.19	
	ACI 318-19	Deflection	2.77	5.51	8.19	10.84	8.19	5.51	2.77			
		[22]	Discrepancies	0.57	0.74	1.84	3.64	1.79	0.66	0.52	1.75	

All deflection values are in mm

Due to the improved assessment accuracy compared to GPS and close-range photogrammetry methods, the proposed method can be used as an efficient and cost-effective solution for structural monitoring, providing many advantages, such as:

- It utilizes simple and low-cost surveying instruments such as theodolite.
- It does not demand pricey GPS receiver antennas or metric or non-metric camera systems.
- It is appropriate for both indoor and outdoor use.
- It is easier in reaching buildings or elements.
- It is simply executed by a surveyor rather than a professional or a photogrammetrist.
- It does not require in situ sensor instrumentation.
- Eliminates wiring-costs.

REFERENCES

- [1] P. Kot, M. Muradov, M. Gkantou, G. S. Kamaris, K. Hashim, and D. Yeboah, "Recent Advancements in Non-Destructive Testing Techniques for Structural Health Monitoring," *Applied Sciences*, vol. 11, no. 6, Jan. 2021, Art. no. 2750, <https://doi.org/10.3390/app11062750>.
- [2] D. González-Aguilera, J. Gómez-Lahoz, and J. Sánchez, "A New Approach for Structural Monitoring of Large Dams with a Three-Dimensional Laser Scanner," *Sensors*, vol. 8, no. 9, pp. 5866–5883, Sep. 2008, <https://doi.org/10.3390/s8095866>.
- [3] W. Mukupa, G. W. Roberts, C. M. Hancock, and K. Al-Manasir, "A review of the use of terrestrial laser scanning application for change detection and deformation monitoring of structures," *Survey Review*, vol. 49, no. 353, pp. 99–116, Mar. 2017, <https://doi.org/10.1080/00396265.2015.1133039>.
- [4] M. Javanpour and P. Zarfam, "Application of Incremental Dynamic Analysis (IDA) Method for Studying the Dynamic Behavior of Structures During Earthquakes," *Engineering, Technology & Applied Science Research*, vol. 7, no. 1, pp. 1338–1344, Feb. 2017, <https://doi.org/10.48084/etasr.902>.
- [5] O. M. Mubarak, "The Effect of Carrier Phase on GPS Multipath Tracking Error," *Engineering, Technology & Applied Science Research*, vol. 10, no. 5, pp. 6237–6241, Oct. 2020, <https://doi.org/10.48084/etasr.3578>.
- [6] K. L. A. El-Ashrawy, "An Efficient Methodology for Detecting the Vertical Movement of Structures," *Engineering, Technology & Applied Science Research*, vol. 13, no. 1, pp. 9913–9918, Feb. 2023, <https://doi.org/10.48084/etasr.5460>.
- [7] M. N. Ono, E. S. O., and O. O. F., "Comparative Analysis of DGPS and Total Station Accuracies for Static Deformation Monitoring Of Engineering Structures," *IOSR Journal of Environmental Science, Toxicology and Food Technology (IOSR-JESTFT)*, vol. 12, no. 6, 2018, Art. no. 19, <https://doi.org/10.9790/2402-1206011929>.
- [8] K. L. A. El-Ashrawy, "Accuracy, time cost and terrain independence comparisons of levelling techniques," *Geodesy and Cartography*, vol. 40, no. 3, pp. 133–141, Jul. 2014, <https://doi.org/10.3846/20296991.2014.962727>.
- [9] J. Zhou, B. Shi, G. Liu, and S. Ju, "Accuracy analysis of dam deformation monitoring and correction of refraction with robotic total station," *PLOS ONE*, vol. 16, no. 5, 2021, Art. no. e0251281, <https://doi.org/10.1371/journal.pone.0251281>.
- [10] I. M. Abdullahi and N. A. Yelwa, "Structural Deformation Monitoring Surveys of New Administrative Building of Federal School of Surveying, Oyo – Nigeria," *International Journal of Science and Technology*, vol. 6, no. 1, Jan. 2016.
- [11] C. D. Ghilani, *Adjustment Computations: Spatial Data Analysis*. Hoboken, NJ, USA: John Wiley & Sons, 2017.
- [12] H. Lahamy, D. D. Lichti, J. Steward, M. El-Badry, and M. Moravvej, "Measurement of Deflection in Concrete Beams During Fatigue Loading Test Using the Microsoft Kinect 2.0," *Journal of Applied Geodesy*, vol. 10, no. 1, pp. 71–77, Mar. 2016, <https://doi.org/10.1515/jag-2015-0023>.
- [13] J. Yu, X. Meng, B. Yan, B. Xu, Q. Fan, and Y. Xie, "Global Navigation Satellite System-based positioning technology for structural health monitoring: a review," *Structural Control and Health Monitoring*, vol. 27, no. 1, 2020, Art. no. e2467, <https://doi.org/10.1002/stc.2467>.
- [14] R. Paar, A. Marendić, I. Jakopc, and I. Grgac, "Vibration Monitoring of Civil Engineering Structures Using Contactless Vision-Based Low-Cost IATS Prototype," *Sensors*, vol. 21, no. 23, Jan. 2021, Art. no. 7952, <https://doi.org/10.3390/s21237952>.
- [15] S. D. Mayunga and M. Bakaone, "The Application of Global Positioning Systems (GPS) and Linear Variable Differential Transducers (LVDT) for Bridge Deformation Monitoring," *Research Developments in Science and Technology Vol. 3*, pp. 109–126, Apr. 2022, <https://doi.org/10.9734/bpi/rdstv3/2125A>.
- [16] N. Manzini *et al.*, "Performance analysis of low-cost GNSS stations for structural health monitoring of civil engineering structures," *Structure and Infrastructure Engineering*, vol. 18, no. 5, pp. 595–611, May 2022, <https://doi.org/10.1080/15732479.2020.1849320>.
- [17] I. Detchev, A. Habib, D. Lichti, and M. El-Badry, "Structural 3D Monitoring Using a New Sinusoidal Fitting Adjustment," *ISPRS Annals of the Photogrammetry, Remote Sensing and Spatial Information Sciences*, vol. III-5, pp. 3–10, Jun. 2016, <https://doi.org/10.5194/isprs-annals-III-5-3-2016>.
- [18] F. Esmaili, H. Ebadi, A. Mohammadzade, and M. Saadatseresh, "Evaluation of Close-Range Photogrammetric Technique for Deformation Monitoring of Large-Scale Structures: A review," *Journal of Geomatics Science and Technology*, vol. 8, no. 4, pp. 41–55, 2019.
- [19] J. J. Wang, N. Gowripalan, J. Li, and V. V. Nguyen, "Close-range photogrammetry for accurate deformation distribution measurement," in *Mechanics of Structures and Materials: Advancements and Challenges - Proceedings of the 24th Australasian Conference on the Mechanics of Structures and Materials, ACMSM24*, 2016, pp. 793–799.
- [20] J. Hu, E. Liu, and J. Yu, "Application of Structural Deformation Monitoring Based on Close-Range Photogrammetry Technology," *Advances in Civil Engineering*, vol. 2021, Feb. 2021, Art. no. e6621440, <https://doi.org/10.1155/2021/6621440>.
- [21] R. Maalek, D. D. Lichti, and J. Y. Ruwanpura, "Automatic Recognition of Common Structural Elements from Point Clouds for Automated Progress Monitoring and Dimensional Quality Control in Reinforced Concrete Construction," *Remote Sensing*, vol. 11, no. 9, Jan. 2019, Art. no. 1102, <https://doi.org/10.3390/rs11091102>.
- [22] Y. Yan and J. F. Hajjar, "Automated extraction of structural elements in steel girder bridges from laser point clouds," *Automation in Construction*, vol. 125, May 2021, Art. no. 103582, <https://doi.org/10.1016/j.autcon.2021.103582>.
- [23] H. Sorin, "Measuring and determinate the dynamic deformation of constructions using modern theologies and techniques," *RevCAD – Journal of Geodesy and Cadastre*, pp. 191–198, 2009.
- [24] M. E. El-Tokhey, A. K. Abdel-Gawad, Y. M. Mogahed, and A. M. El-Maghraby, "Accuracy Assessment of Laser Scanner in Measuring and Monitoring Deformations of Structures," *World Applied Sciences Journal*, vol. 26, no. 2, pp. 144–151, 2013.
- [25] "Building Code Requirements for Structural Concrete (ACI 318-19) and Commentary," American Concrete Institute, Standard ACI 318-19, 2019.
- [26] K. L. A. El-Ashrawy, "Developing and testing a method for deformations measurements of structures," *Geodesy and Cartography*, vol. 43, no. 1, pp. 35–40, Jan. 2017, <https://doi.org/10.3846/20296991.2017.1305545>.
- [27] E. M. Mikhail and F. E. Ackermann, *Observations and least squares*. New York, NY, USA: IEP, 1976.
- [28] J. Santos and A. A. Henriques, "Span-to-depth ratio limits for RC continuous beams and slabs based on MC2010 and EC2 ductility and deflection requirements," *Engineering Structures*, vol. 228, Feb. 2021, Art. no. 111565, <https://doi.org/10.1016/j.engstruct.2020.111565>.

- [29] C. Mancuso and F. M. Bartlett, "ACI 318-14 Criteria for Computing Instantaneous Deflections," *Structural Journal*, vol. 114, no. 5, pp. 1299–1310, Sep. 2017, <https://doi.org/10.14359/51689726>.
- [30] P. H. Bischoff and A. Scanlon, "Span-Depth Ratios for One-Way Members Based on ACI 318 Deflection Limits," *Structural Journal*, vol. 106, no. 5, pp. 617–626, Sep. 2009, <https://doi.org/10.14359/51663102>.
- [31] N. J. Gardner, "Span/Thickness Limits for Deflection Control," *Structural Journal*, vol. 108, no. 4, pp. 453–460, Jul. 2011, <https://doi.org/10.14359/51682985>.
- [32] P. Sarkar, M. Govind, and D. Menon, "Estimation of short-term deflection in two-way RC slab," *Structural Engineering and Mechanics*, vol. 31, no. 2, pp. 237–240, Jan. 2009, <https://doi.org/10.12989/SEM.2009.31.2.237>.
- [33] B. Vakhshouri and S. Nejadi, "Effect of fiber reinforcing on instantaneous deflection of self-compacting concrete one-way slabs under early-age loading," *Structural Engineering and Mechanics*, vol. 67, no. 2, pp. 155–163, Jan. 2018.
- [34] L. M. Gil-Martina and E. Hernandez-Montes, "Review of the reinforcement sizing in the strength design of reinforced concrete slabs," *Computers and Concrete*, vol. 27, no. 3, pp. 211–223, 2021, <https://doi.org/10.12989/cac.2021.27.3.211>.
- [35] F. Ding, W. Wang, B. Jiang, L. Wang, and X. Liu, "Numerical analysis of simply supported one-way reinforced concrete slabs under fire condition," *Computers and Concrete*, vol. 27, no. 4, pp. 355–367, 2021, <https://doi.org/10.12989/cac.2021.27.4.355>.
- [36] W. Sun, Y. Zhou, J. Xiang, B. Chen, and W. Feng, "Crack detection in concrete slabs by graph-based anomalies calculation," *Smart Structures and Systems*, vol. 29, no. 3, pp. 421–431, 2022, <https://doi.org/10.12989/sss.2022.29.3.421>.
- [37] Z. Sakka and R. I. Gilbert, "Numerical investigation on the structural behavior of two-way slabs reinforced with low ductility steel," *Structural Engineering and Mechanics*, vol. 65, no. 3, pp. 223–231, 2018, <https://doi.org/10.12989/sem.2018.65.3.223>.
- [38] A. A. Yaseen and A. A. Abdul-Razzak, "New constitutive models for non linear analysis of high strength fibrous reinforced concrete slabs," *Structural Engineering and Mechanics*, vol. 82, no. 1, pp. 121–131, 2022, <https://doi.org/10.12989/sem.2022.82.1.121>.
- [39] G. Nistor, "Direct Algorithm for the Calculation of Vertical Displacements and Deformations of Constructions Using High-Precision Geometric Leveling," *Cadastre Journal RevCAD*, pp. 11–18, Jul. 2017.